*Int. J. Solids Structures* Vol. 30, No. 24, pp. 3417–3429, 1993
Printed in Great Britain

0020–7683/93 $6.00+ .00
Pergamon Press Ltd

# THE EFFECT OF FIBER DAMAGE ON THE LONGITUDINAL CREEP OF A CFMMC

KEVIN W. KELLY
Science Applications International Corporation

and

EVER BARBERO
Mechanical and Aerospace Engineering, West Virginia University, Norgantown, WV 25506, U.S.A.

(*Received* 29 *September* 1992; *in revised form* 14 *June* 1993)

**Abstract**—Fiber failures which may exist in a continuous fiber composite before the composite is loaded or generated while the composite is loaded, introduce an additional strain component not included in existing continuous fiber models. Equations are developed which can be used to calculate the magnitude of this additional strain. A Finite Element Model (FEM), in the form of a Representative Volume Element (RVE), calculates the stress field surrounding a fiber break. Statistical analysis is used to infer the behavior of a large composite sample from the stress analysis of a single break. The creep strain, the time to failure, and time-dependent composite strength can all be calculated by combining the FEM results, the statistical analysis model, and knowledge of the initial average fiber length. Important variables included in the calculation are process-related parameters such as the fiber–matrix interface strength and roughness.

## INTRODUCTION

Continuous fiber–metal matrix composites (CFMMCs) are seen as attractive material candidates in applications where high strength or stiffness-to-weight ratios at relatively high temperature are required. Their ability to succeed commercially depends upon whether their material properties, particularly in the longitudinal direction, are both well understood and superior to other candidate materials. The longitudinal creep of a CFMMC is one of the important material properties which must be well understood if these materials are to be used in moderately high temperature applications where tight physical tolerances exist.

The longitudinal creep of a CFMMC with no fiber breaks can be accurately predicted by analytic models (McLean, 1983; Aboudi, 1991). Different assumptions are made for different combinations of matrix and fiber creep behavior. This paper focuses on composites with creeping metal matrix and elastic fibers of finite length. The analytic model of McLean, which addresses the creep behavior of CFMMC with no fiber breaks, makes the following assumptions: the longitudinal strain of both the fiber and matrix are assumed to be identical; Poisson effects are negligible; and the matrix creep rate is governed by a power law. When a constant longitudinal stress is applied to the composite, the matrix creeps, the stress in the fibers increases, and simultaneously, the matrix stress (and matrix creep rate) decreases. The creep strain rate approaches zero when the stress in the matrix becomes negligible. Figure 1 shows the model's prediction of the longitudinal creep of a Titanium 6-4 matrix alumina–fiber composite with a 30% fiber volume when subjected to a 689.4 MPa (100 ksi) longitudinal stress. The constituent properties used are given in Appendix 1. The creep rate following the load application is controlled by the matrix creep law. The steady state strain and fiber stress, however, are only functions of the fiber properties and percent fiber volume and can be calculated using the equations below:

$$\varepsilon_{\infty} = \frac{\sigma_c}{E_F V_F}, \tag{1}$$

$$\sigma_F = \frac{\sigma_c}{V_F}, \tag{2}$$

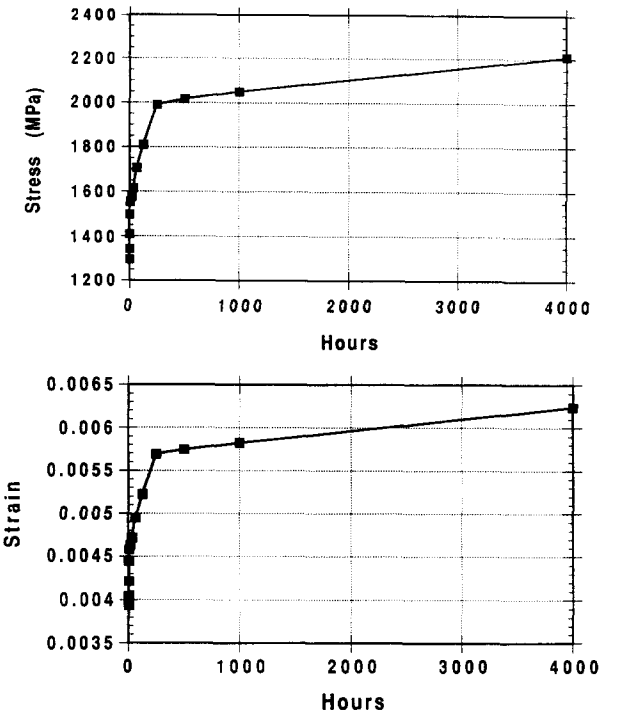


Fig. 1. Predictions of continuous fiber model (427°C).

where $\varepsilon_\infty$ = steady state strain,
$\sigma_c$ = composite stress,
$E_F$ = fiber elastic modulus,
$V_F$ = percent fiber volume,
$\sigma_F$ = steady state fiber stress.

If there are fiber breaks in a composite, it is no longer "continuous". Fiber breaks may exist in the composite before a load is applied (introduced during processing), or they may be generated in response to an applied load. In either case, a fiber break causes a local composite compliance increase. Analytic models that predict the stiffness decrease caused by fiber failures have been developed. Steif (1984), for example, shows that the magnitude of the stiffness change associated with each fiber failure is a function of the constituent properties and the ineffective length $\delta$ (Fig. 2) over which the fiber can be considered unloaded at a fiber break. His model, however, cannot predict the strength of the composite (maximum strain) or time-dependent strains associated with creep. Kelly and Street (1972)

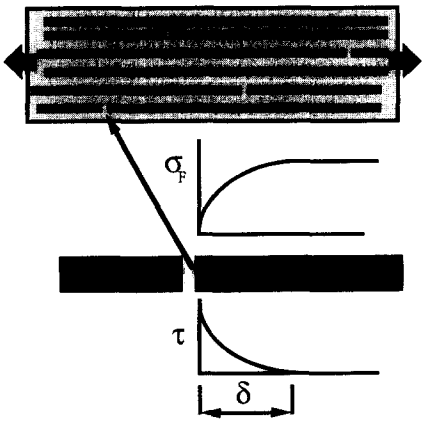


Fig. 2. Definition of ineffective length $\delta$.

developed an analytic model which predicts the creep of a composite with a given constant average fiber length. However, when a load is applied to an MMC at high temperatures, matrix relaxation can cause additional fiber failures (and the average fiber length to decrease), as well as magnify the stiffness loss accompanying each fiber break. Lifshitz and Rotem (1970) also modeled composite creep analytically. Their analysis does include the effects of stress-induced fiber failure, but it does not include pre-existing fiber breaks. In addition, their assumption that the fiber–matrix interface strength is infinite leads to predictions of strengths which are far too high in many composites where the interface strength is weak. In summary, existing creep models do not provide the ability to account for both pre-existing fiber breaks as well as stress-induced fiber damage, and predict time-dependent composite strength or the strain associated with creep rupture.

This paper presents a model to predict how randomly-spaced fiber failures affect longitudinal creep. Given an assumed initial average fiber length (fiber break density), the model is able to calculate the number of additional fiber failures induced by the combination of a constant applied load and matrix relaxation, the additional creep strain associated with calculated fiber break density, and the time to creep rupture.

## STATISTICAL ANALYSIS

The strength of many elastic fibers is a function of the gauge length used during strength tests. However, the length scale which controls the strength of fibers in a composite is the length over which a fiber recovers a large percentage of its load (90%) near a fiber break and not the specimen length (Fig. 2). This length, $\delta$, is often called the ineffective length. Rosen (1964) recognized this fact and proposed that the longitudinal ultimate strength of fibers in a ductile-matrix, elastic-fiber composite can be accurately predicted by the strength of a dry bundle of length $\delta$.

A "dry" fiber is defined, in this paper, as a number of parallel fibers of some given length and diameter which, if unbroken, carry the same load. After a fiber within a dry bundle fails, the load it carried is shared equally by the remaining unbroken fibers. A dry bundle typically refers to fibers which have not yet been combined with matrix. As tensile load is slowly applied to a dry bundle of fibers which have some distribution of strength, the weaker fibers (with large flaw sizes) begin to fail and the stress on the remaining unbroken fibers increases accordingly. The Weibull expression (Weibull, 1951), often used to describe the cumulative probability, $F(\sigma)$, that a fiber of length $\delta$ will fail at stress $\sigma$, is given as

$$F(\sigma) = 1 - \exp\left[\frac{-\delta}{L_0}\left(\frac{\sigma}{\sigma_0}\right)^m\right]. \tag{3}$$

The values of $\sigma_0$ and $m$, which represent the characteristic strength of the fiber, and the dispersion of fiber strength, respectively, can be determined from fiber strength experiments. $L_0$ is the characteristic gauge length corresponding to stress, $\sigma_0$. Equation (3) can be simplified as shown below:

$$\alpha = \frac{1}{L_0\sigma_0^m}, \tag{4}$$

$$F(\sigma) = 1 - \exp\left[-\delta\alpha\sigma^m\right]. \tag{5}$$

Quite often, fiber vendors provide the average strength, $\sigma_{av}$, for a given gauge length $L$, rather than $\alpha$. In these cases, eqn (6) can be used to calculate the value of $\alpha$:

$$\alpha = \left[\frac{\Gamma\left(1+\frac{1}{m}\right)}{\sigma_{uu}}\right]^m \frac{1}{L}. \tag{6}$$

If no fiber breaks exist initially in the composite, eqn (5) provides the percentage of fibers in a bundle which are broken as a function of the stress in the unbroken fibers. However, if there are randomly distributed fiber breaks in the composite prior to loading, the total percentage of broken fibers in each $\delta$-long bundle will be greater than predicted by eqn (5). A more general expression of the percentage of broken fibers is given by eqn (7), where $L_i$ is the average initial fiber length. The subscript "t" is used to differentiate the total damage from the damage associated with stress-induced fiber failure provided by eqn (5):

$$F_t(\sigma) = [1-\exp(-\delta\alpha\sigma^m)]\left(1-\frac{\delta}{L_i}\right)+\frac{\delta}{L_i}. \tag{7}$$

The first term on the right-hand side represents the percentage of fibers which can be considered initially unbroken, but which fail at stress $\sigma$, while the second term is the percentage of fibers that can be considered initially broken. The percentage of fibers which are unbroken, $1-F_t(\sigma)$, is given as

$$1-F_t(\sigma) = \exp(-\delta\alpha\sigma^m)\left(1-\frac{\delta}{L_i}\right). \tag{8}$$

The bundle stress, $\sigma_b$, is equal to the applied load divided by the total fiber cross-sectional area, or average fiber stress. It is also equal to the product of the stress in unbroken fibers, $\sigma$, and the percentage of fibers which are unbroken:

$$\sigma_b = \sigma\left[\exp(-\delta\alpha\sigma^m)\left(1-\frac{\delta}{L_i}\right)\right]. \tag{9}$$

The value of $\sigma$ which maximizes eqn (9), $\sigma_m$, can be easily determined and is given in eqn (10). This critical stress is not a function of the percentage of fibers which are considered initially unbroken:

$$\sigma_m = (\delta\alpha m)^{-1/m}. \tag{10}$$

The maximum (or critical) bundle stress, $\sigma_c$, which can be determined by combining eqns (9) and (10), is given by eqn (11), $\sigma_c$ is often called the bundle strength:

$$\sigma_c = \left[1-\frac{\delta}{L_i}\right](\delta\alpha me)^{-1/m}. \tag{11}$$

The critical or maximum damage, $F_{cr}$, which provides the percentage of fibers in a bundle which are broken prior to catastrophic failure, is given below [obtained by combining eqns (7) and (10)]:

$$F_{cr} = \left[1-\exp\frac{-1}{m}\right]\left(1-\frac{\delta}{L}\right)+\frac{\delta}{L}. \tag{12}$$

If $\delta$ and $F(\sigma)$ are known, the average fiber length within the composite, $L_{av}$, is easily calculated using eqn (13). The average fiber length differs from the initial average fiber length because of load-induced fiber failures:

$$L_{av} = \frac{\delta}{F_t(\sigma)}. \tag{13}$$

Rather than represent the composite as a series of bundles $\delta$ in length, the composite may also be considered a collection of cylinders, each containing a single broken fiber as shown in Fig. 3. A cylinder with a volume equal to the average volume of the cylinders shown in Fig. 3 can be considered a representative volume element (RVE). The total length of fiber contained in the RVE is equal to the average fiber length in the composite (neglecting end effects). Therefore, the volume of the RVE, $V_{RVE}$, is simply the volume associated with a fiber of average length, $L_{av}$, divided by the fiber volume fraction:

$$V_{RVE} = \frac{L_{av}\pi D^2}{4V_F}, \tag{14}$$

where $V_{RVE}$ = volume of RVE,
$D$ = fiber diameter,
$V_F$ = fiber volume fraction.

As the matrix creeps, the following sequence occurs: the stress on the fibers increases, fibers break, the average fiber length within the composite decreases, and the size of the RVE decreases to reflect the increased amount of damage. As the RVE volume decreases, the longitudinal strain corresponding to a given applied load increases because the effects of the broken fiber in the center become proportionately larger. Theoretically, the effect of fiber breaks could be calculated numerically by determining the longitudinal strain in an RVE whose volume is continuously decreasing to account for accumulating damage. Fortunately, because neither the bundle stress, $\sigma_b$, nor the ineffective length, $\delta$, are functions of the RVE volume, a method exists, which will be described, to calculate the composite strain using simulation results from an RVE of constant volume. The RVE volume can be chosen arbitrarily, with the stipulation that it be long and tall enough to prevent its boundaries from significantly altering the stress field surrounding a fiber break. It will be shown that the evolution of the average fiber length (or RVE volume), as well as creep strain can be easily calculated if the bundle stress, $\sigma_b$, the ineffective length, $\delta$, and the initial average fiber length are known. While the time-dependent value of $\sigma_b$ can be accurately determined using analytic models, the time-dependent prediction of $\delta$ often requires a numerical model.

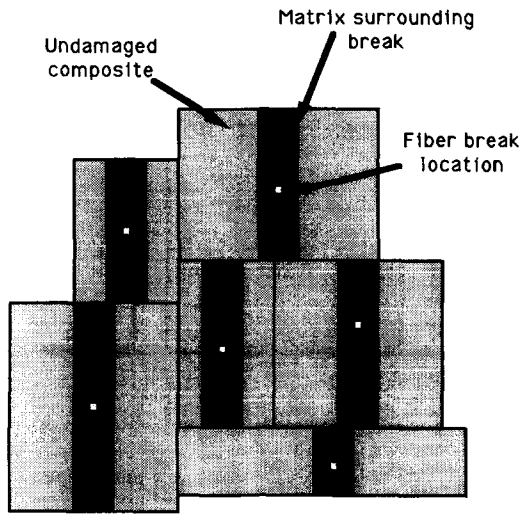


Fig. 3. Model of composite as cylinders containing a fiber break.

## NUMERICAL MODEL

A FEM using ANSYS (1991) has been developed to calculate the response of a composite under longitudinal tension on a RVE containing one internal fiber break. The model calculates the values of $\delta$, the fiber bundle stress, $\sigma_b$, and the average longitudinal strain as functions of time.

The numerical analysis will present modeling results of a titanium matrix, alumina-fiber composite. The alumina fibers have 140 $\mu$m diameters which are representative of single crystal Saphikon fibers. The properties of both the matrix and the fiber used in the model are listed in Appendix 1.

An axisymmetric view of the finite element model is shown in Fig. 4. This is the typical configuration suggested by the cylindrical assemblage model (Hashin and Rosen, 1964; Christensen, 1979; Mikata and Taya, 1985; Hill, 1965). A ring of matrix material surrounds the fiber. The thickness of the matrix ring corresponds to a composite with a 30% fiber volume. In this paper, only coulomb friction resists sliding at the fiber–matrix interface. Sliding occurs when shear at the interface exceeds the product of the compressive force across the interface and the coefficient of friction (Appendix 1). A ring of material with homogenized properties of the undamaged composite is coaxially located outside of and rigidly connected to the ring of matrix. The properties of the homogenized composite are those of the undamaged material (no fiber breaks). The boundary conditions which are used in the model corresponding to Fig. 4 are described as follows:

1. The model is axisymmetric.
2. The bottom surface of both the matrix and undamaged composite cylinders allows zero axial displacement. When the fiber is considered unbroken, its bottom surface allows no axial displacement. When the fiber is considered broken, the bottom surface of the fiber is allowed to move in the positive $z$-direction, but not in the negative.
3. The top surface of the model remains planar in response to longitudinal loads.
4. There are no restraints to radial displacements except along the centerline of the fiber.

## HOMOGENIZED PROPERTIES OF UNDAMAGED COMPOSITE

The success of modeling the stress field surrounding a fiber break hinges on accurately modeling the behavior of the undamaged composite. The composite properties $E_1$, $E_2$, $CTE_1$, $CTE_2$, $G_{21}$, $\nu_{21}$, as well as creep response are needed to predict the response of the

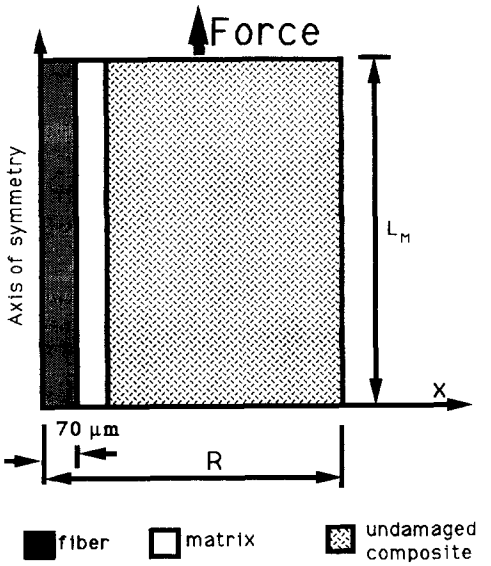


Fig. 4. Model of the RVE.

composite to thermal and mechanical loading. The homogenized composite properties (with the exception of the creep response) were determined using micromechanics (Agarwal and Broutman, 1990; Everett, 1991; Taya, 1989).

## CREEP RESPONSE OF UNDAMAGED COMPOSITE

Analytic expressions (McLean, 1983; Aboudi, 1991) or FEM simulations can be used to estimate the creep in a composite with elastic fibers and creeping matrix subjected to a constant longitudinal load. A constitutive equation relating matrix stress to the creep rate governs the initial slope of the creep displacement versus time plot, and a steady state creep strain is achieved after the load initially carried by the matrix is transferred to the fibers. The longitudinal creep of a continuous titanium-matrix, alumina-fiber composite with a 30% fiber volume fraction subjected to different constant axial stress was calculated using a model similar to that shown in Fig. 4, except that the undamaged composite was not present and the fiber was unbroken. The creep of the matrix was modeled by the equation and constants listed in Appendix 1. The longitudinal creep versus time was calculated for different applied stresses. The results are shown in Fig. 5 and compare identically with analytic expressions if the same matrix creep law is used.

From Fig. 5, it is clear that the steady-state creep strain is directly proportional to the applied stress. In addition, the curves shown in Fig. 5 appear to be of similar shape and differ only by a scale that is proportional to the applied stress. Therefore, the creep strain for any constant applied stress can be closely approximated by eqn (15) below:

$$\varepsilon_{cp}t) = \varepsilon_0(t)\left(\frac{\sigma_a}{\sigma_0}\right), \tag{15}$$

where $\varepsilon_{cp}(t)$ = creep strain,
$\varepsilon_0(t)$ = reference creep strain,
$\sigma_a$ = applied composite stress,
$\sigma_0$ = reference applied composite stress.

The longitudinal creep response of the homogenized composite to any applied load can be closely approximated by adapting constitutive equations which ANSYS provides. The creep strain curve corresponding to an applied composite stress of 551 MPa (80 ksi) was chosen to represent the function $\varepsilon_0(t)$.

The stress state within the undamaged composite is triaxial and its creep response is anisotropic. The creep model is only expected to accurately predict undamaged composite

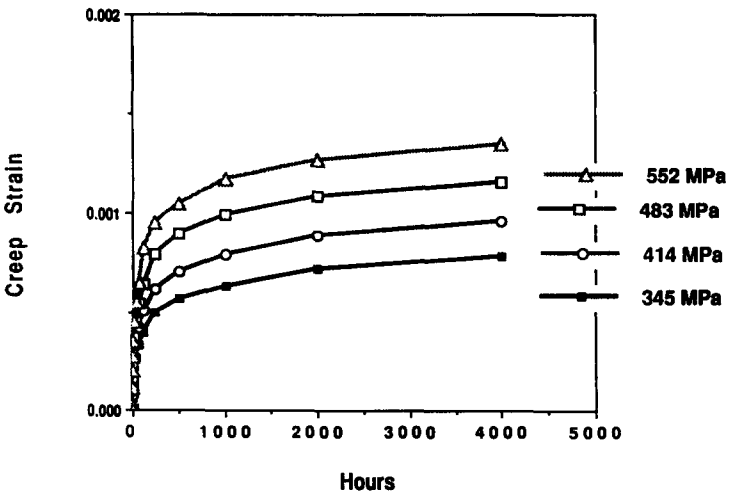


Fig. 5. Axial creep of undamaged composite at 427°C.

creep strain when it is subjected to a pure axial stress. Furthermore, the function $\varepsilon_0(t)$ applies when the applied load is constant. If the stresses within a region of the undamaged composite vary significantly over the time during which load is applied, then the model may not correctly predict the local creep rate. For example, if the stress within a region of the undamaged composite increases with time, the model may underpredict the local creep rate. Nevertheless, the authors believe that the model should represent reasonably well the creep response of the undamaged composite since axial stress dominates and the variation of the stress magnitude within the undamaged composite is relatively small.

## NUMERICAL MODEL RESULTS

Numerical simulations of the model described in Fig. 4 were performed assuming coefficient of friction values, $\mu$, at the fiber–matrix interface of either 0.33 and 1.0. These two values of $\mu$ are used to simulate, respectively, either a weak or strong interfacial shear strength. In either case, cooldown from 927 to 427°C is simulated. Next, a 689.4 MPa (100 ksi) stress is applied and held constant for 4000 hours.

Following cooldown, a radial compressive stress of approximately 65 MPa exists initially at the fiber–matrix interface as a result of residual stresses resulting from cooldown. This compressive stress, combined with the assumed coefficient of friction value, provides the necessary shear stress which must be overcome for slip to occur at the fiber–matrix interface. When a coefficient of friction of 1.0 is assumed, the initial interfacial shear strength is 65 MPa. This value corresponds to a strong interface. Similarly, when the coefficient value is 0.33, the interface strength is proportionately lower (23.3 MPa). This value is typical of fairly weakly bonded interfaces. Over the 4000 hr period of load application, the compressive stress at the interface decreases by about 50% (matrix relaxation) which causes the interface strength, in either case, to decrease accordingly.

The bundle stress, $\sigma_b$, provided by the axial stress in the fiber near the top of the model, is not a function of the value of the coefficient of friction. The bundle stress increases from 1296 to 2213 MPa over the 4000 hr span.

The ineffective length depends on the interface shear strength (coefficient of friction) and the stress on the fibers. A simple axial force balance on the fiber over length $d$ can be used to predict that the value of $\delta$ should be proportional to the maximum stress in the fiber and inversely proportional to the value of $\mu$. Numerical simulations were performed which verified these dependencies. Numerical model results, showing the axial and shear stress fields which exist around a fiber break immediately after the load was applied and 4000 hr after the load was applied are shown in Figs 6 and 7. The coefficient of friction used in Figs 6 and 7 was 1.0. It is convenient to express $\delta$ as some multiple of the fiber diameter $D$. The time-dependent values of $\delta$ for coefficient of friction values of 0.33 and 1.0 are shown in Fig. 8. Also shown in Fig. 8 is the time dependent value of $\sigma_b$.

## DISCUSSION

When a load is applied to a composite, each fiber segment carries "full" load over its entire length except near each end. At each end, the stress increases from a value of zero at the break to the "full" value over length $\delta$. If the stress is assumed to increase linearly over the ineffective length, and if the average fiber length in the composite equals $L_{av}$, then the percentages of fiber within the composite which can be considered loaded and unloaded respectively, are given by eqns (16) and (17):

$$\% \text{ Fully Loaded} = 1 - \frac{\delta}{L_{av}}, \tag{16}$$

$$\% \text{ Fully Unloaded} = \frac{\delta}{L_{av}}. \tag{17}$$

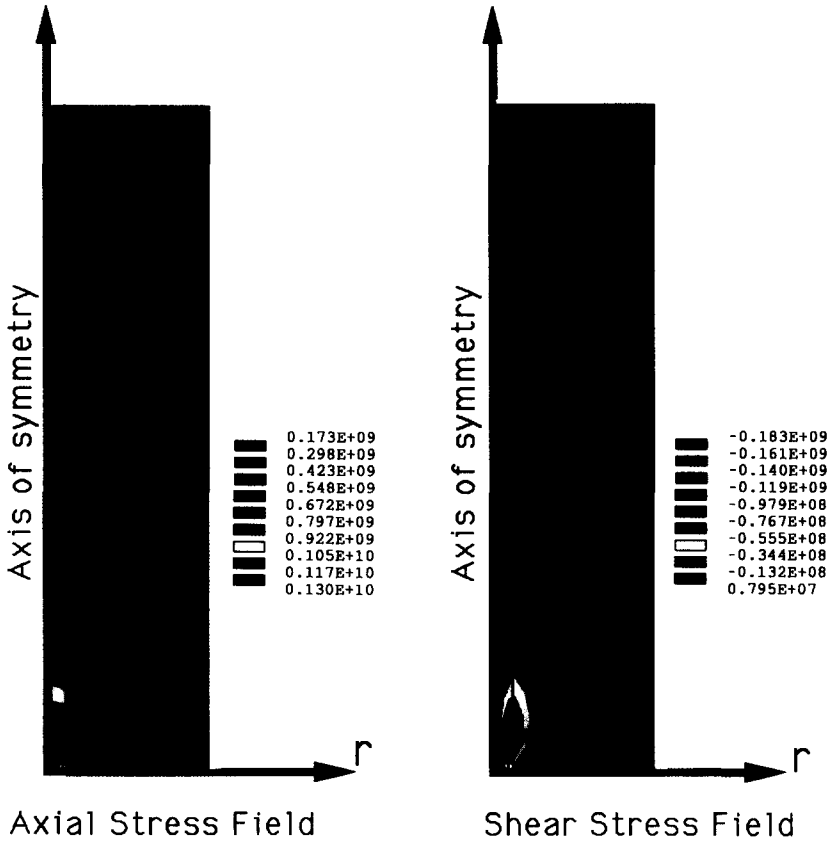


Fig. 6. Stress fields immediately after 689 MPa load applied, $\mu = 1.0$.

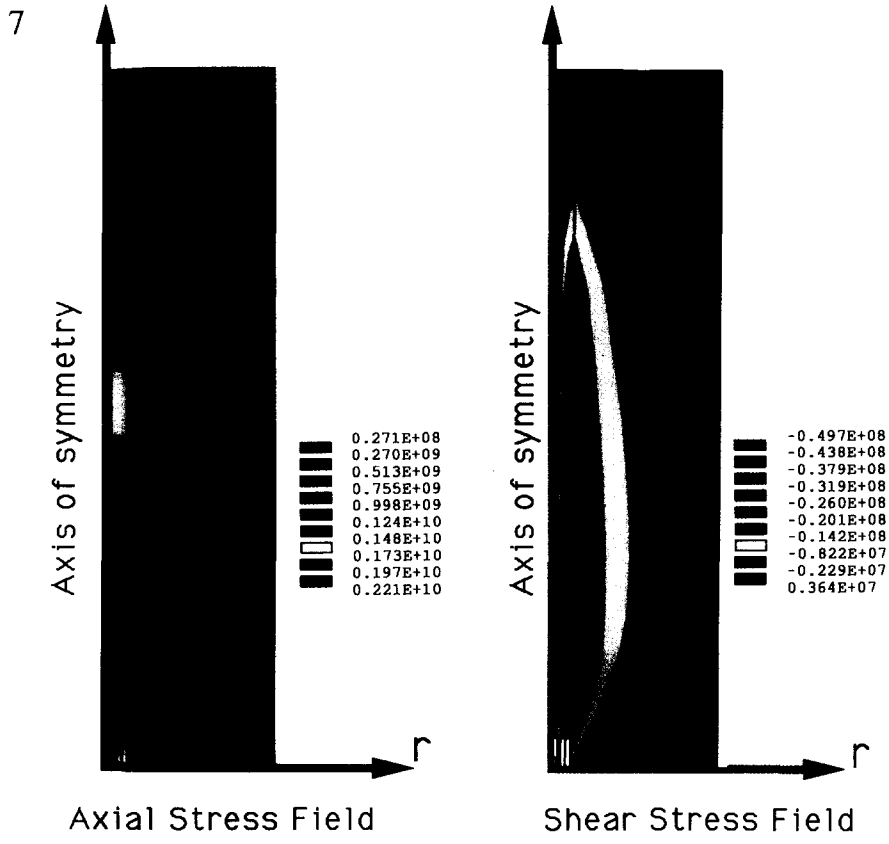


Fig. 7. Stress fields after 689 MPa stress applied for 4000 hr, $\mu = 1.0$.

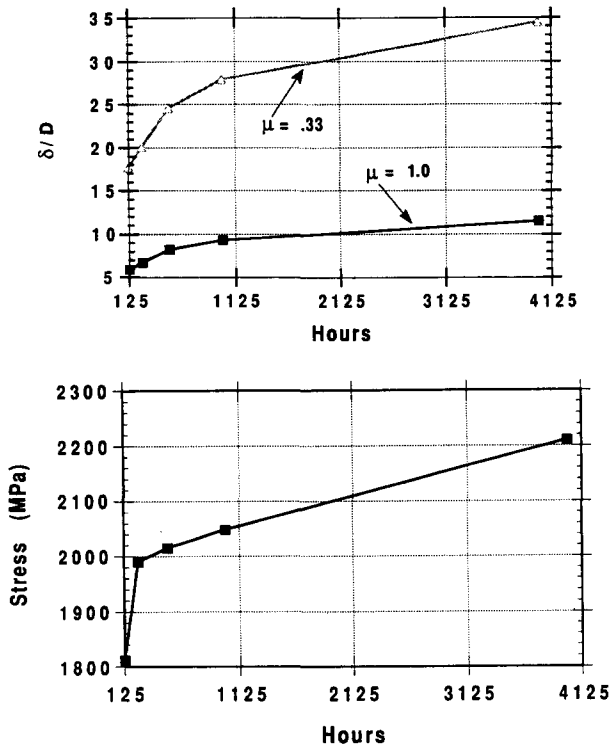


Fig. 8. Fiber bundle stress and $\delta$ versus time.

If the composite is modeled as a series of bundles of length $\delta$, then the percentage of fibers in each bundle which are unbroken is given by eqn (16). The composite strain is always equal to the strain in the unbroken fibers of a fiber bundle. This strain, $\varepsilon$, is equal to the stress in the unbroken fibers divided by the fiber elastic modulus. The stress in the unbroken fibers is equal to the applied fiber bundle stress divided by the percentage of fibers which are unbroken. The resulting relationship between the composite strain, $\varepsilon$, and the fiber bundle stress, $\sigma_b$ is given by eqn (18a). Note that by setting the ratio of $\delta/L_{av}$ to zero, the time dependent strain of a continuous fiber composite is obtained. Equation (18a) is valid at any time because the value of $\sigma_b$ includes the effects of matrix relaxation:

$$\varepsilon = \frac{\sigma_b}{E_F\left(1 - \dfrac{\delta}{L_{av}}\right)}. \tag{18a}$$

By combining eqns (18a) and (13), eqn (18b) is obtained:

$$\varepsilon = \frac{\sigma_b}{E_F(1 - F_t)}. \tag{18b}$$

A known time-dependent $\sigma_b$–$\delta$ combination (provided by the FEM), coupled with the initial average fiber length, can be used to calculate corresponding values of the bundle strength ($\sigma_c$) [eqn (11)], the stress in unbroken fibers ($\sigma$) [eqn (9)], the percentage of broken fibers, $F_t(\sigma)$ [eqn (7)], the average fiber length ($L_{av}$) [eqn (13)], and strain [eqn (18b)]. Tables 1(a, b and c) provide the values of these parameters based on the values of $\sigma_b$–$\delta$ provided by Fig. 8 (using the $\delta$ values corresponding to $\mu = 0.33$) and three assumed initial average fiber lengths ($L_i/D = \infty$, $L_i/D = 500$, $L_i/D = 200$). Tables such as these can be used to predict the time-dependent creep and the time-to-creep rupture of a composite with a given initial average fiber length, interface properties and fiber diameter. These tables also

Table 1(a). $L_i = \infty$
($m = 9$, $\alpha = 2.7\text{E-}32$, $D = 140\ \mu\text{m}$)

| Time | $\sigma_b$ (MPa) | $\delta/D$ | $\sigma_c$ (MPa) | $\sigma$ (MPa) | $F_t(\sigma)$ | $L_{av}/D$ |
|---|---|---|---|---|---|---|
| 125 | 1813 | 17.0 | 2646 | 1814 | 0.00137 | 12,408 |
| 250 | 1964 | 20.1 | 2597 | 1970 | 0.0034 | 5911 |
| 500 | 2025 | 24.6 | 2540 | 2035 | 0.00555 | 4432 |
| 1000 | 2061 | 27.9 | 2503 | 2075 | 0.0075 | 3720 |
| 4000 | 2213 | 34.5 | 2446 | 2240 | 0.0183 | 1885 |

Table 1(b). $L_i = 500\ D$
($m = 9$, $\alpha = 2.7\text{E-}32$, $D = 140\ \mu\text{m}$)

| Time | $\sigma_b$ (MPa) | $\delta/D$ | $\sigma_c$ (MPa) | $\sigma$ (MPa) | $F_t(\sigma)$ | $L_{av}/D$ |
|---|---|---|---|---|---|---|
| 125 | 1813 | 17.0 | 2556 | 1880 | 0.0359 | 473 |
| 250 | 1964 | 20.1 | 2493 | 2060 | 0.0451 | 451 |
| 500 | 2025 | 24.6 | 2413 | 2150 | 0.0577 | 436 |
| 1000 | 2061 | 27.9 | 2362 | 2220 | 0.0687 | 406 |
| 4000 | 2213 | 34.5 | 2277 | 2500 | 0.1141 | 302 |

Table 1(c). $L_i = 200\ D$
($m = 9$, $\alpha = 2.7\text{E-}32$, $D = 140\ \mu\text{m}$)

| Time | $\sigma_b$ (MPa) | $\delta/D$ | $\sigma_c$ (MPa) | $\sigma$ (MPa) | $F_t(\sigma)$ | $L_{av}/D$ |
|---|---|---|---|---|---|---|
| 125 | 1813 | 17.0 | 2421 | 1990 | 0.877 | 193.8 |
| 250 | 1964 | 20.1 | 2336 | 2205 | 0.1085 | 185 |
| 500 | 2025 | 24.6 | 2227 | 2355 | 0.1409 | 174 |
| 1000 | 2061 | 27.9 | 2152 | 2500 | 0.1730 | 161 |
| 4000 | 2213 | 34.5 | 2025 | — | — | — |

provide a relative measure of the longitudinal creep that will exist in a composite containing damage compared to the creep of a continuous fiber composite. For example, if the initial average fiber length of the composite described in Fig. 4 is $200D$, after 1000 hr, the strain will be 20.7% greater than predicted by a continuous fiber model [based on the values provided by Table 1(c) and eqn (18b)]. Between 1000 and 4000 hr, creep rupture will occur (the bundle stress, $\sigma_b$, becomes greater than the bundle strength, $\sigma_c$). If the average initial composite length is $500D$, then after 4000 hr, creep rupture will not have occurred and composite creep will be 12.9% greater than predicted for a continuous fiber model. Finally, over the 4000 hr period, the average length of the composite with no assumed initial fiber breaks decreases to a finite length because of stress-induced fiber failure. However, the composite strain is almost identical to that predicted for the continuous fiber model.

Implicit in the above methodology is the assumption that the stress field around every fiber break is identical. Those fibers which break soon after load is applied are expected to have different ineffective lengths $\delta$ than breaks which occur much later in time. The primary causes of the ineffective length increase with time are the increasing load on the fibers and relaxation of the compressive stress at the fiber–matrix interface due to matrix creep. Both of these processes occur everywhere in the composite at a rate that is somewhat insensitive to proximity to a fiber break location. Therefore, at least when coulomb friction provides transfer of shear across the interface, it is likely that the ineffective lengths around fiber break locations are relatively insensitive to the sequence of breaks.

## CONCLUSIONS

A numerical model is used to calculate the time-dependent values of the fiber bundle stress, $\sigma_b$, and the ineffective length, $\delta$. While the bundle stress can be estimated analytically, a numerical model provides a greatly enhanced capability to account for many parameters that influence the growth of $\delta$.

A set of equations is introduced which can be used to calculate the time-dependent strain, time to rupture, and the time-dependent strength of a composite, given the time-dependent $\sigma_b$–$\delta$ combination. In addition, the accuracy of the simple continuous fiber model creep prediction can be easily determined. Finally, the ability to determine the relative importance of many parameters on strength and creep response is provided.

*Acknowledgements*—Provision of the ANSYS finite element program and technical support by Swanson Analysis Systems of Washington, PA was greatly appreciated. The research was sponsored by DARPA and 3M contract MDA972-90-C-018.

## REFERENCES

Aboudi, J. (1991). *Mechanics of Composite Materials*. Elsevier, NY.
Agarwal, B. D. and Broutman, C. J. (1990). *Analysis and Performance of Fiber Composites*. John Wiley, NY.
ANSYS (1991). *Theoretical Manual, Revision 4.4*. Swanson Analysis Systems Inc., Houston, PA.
Christensen, R. and Lo, K. (1979). Solutions for effective shear properties in three phase sphere and cylinder models. *J. Mech. Phys. Solids* **27,** 315–330.
Deve, H. (1992). Personal communication. 3M Corporation, St Paul, MN.
Everett, R. K. and Arsenault, R. J. (1991). *Metal Matrix Composites: Mechanisms and Properties*. Academic Press, Boston.
Hashin, Z. and Rosen, B. W. (1964). The elastic moduli of fiber-reinforced materials. *J. Appl. Mech.* **31,** 232.
Hill, R. (1965). Theory of mechanical properties of fiber-strengthened materials: III. Self-consistent model. *J. Mech. Phys. Solids* **13,** 198.
Kelly, A. and Street, K. (1972). Creep of discontinuous fiber composites. *Proc. Roy. Soc. Lond.* **A328,** 283–293.
Lifshitz, J. and Rotem, A. (1970). Time-dependent longitudinal strength of unidirectional fibrous composites. *Fiber Sci. Technol.* **3,** 1–21.
McLean, M. (1983). *Directionally Solidified Materials for High Temperature Service*. The Metal Society, London.
*Metals Handbook* (1961). (8th Edn, Vol. 1). American Society for Metals, Novelty, OH.
Mikata, Y. and Taya, M. (1985). Stress field in a coated continuous fiber composite subjected to thermo-mechanical loadings. *J. Compos. Mater.* **19,** 554–578.
Nimmer, R. P., Bankert, R. J., Russell, E. S. and Smith, G. A. (1989). Micromechanical modeling of fiber/matrix interface effects in SiC/Ti metal matrix composites. *Proc. 1989 ASM Materials Week*, Indianapolis, IN, 2 October 1989.
Rosen, B. W. (1964). The tensile failure of fibrous composites. *AIAA Jl* **2**(11), 1985–1991.
Steif, P. (1984). Stiffness reduction due to fiber breakage. *J. Compos. Mater.* **17,** 153–172.
Taya, M. and Arsenault, R. (1989). *Metal Matrix Composites*. Pergamon Press, Oxford.
Weibull, W. (1951). A statistical distribution function of wide applicability. *J. Appl. Mech.* **18,** 293–296.
Wright, P. K., Russell, E., Nimmer R. and Smith, G. (1989). Creep in Ti/SiC composites. Presented at TVIS Annual Meeting, Las Vegas, Nevada, 27 February–2 March 1989.

## APPENDIX 1

*Properties of Ti 6-4 at 427°C*

| | |
|---|---|
| Elastic Modulus† | 87.5 GPa, |
| Poisson Ratio‡ | 0.3, |
| CTE§ | 10.44 E-6°C$^{-1}$, |
| Shear Modulus‡ | GPa, |
| Yield Strength† | 496 MPa, |
| Creep equation‖ | $d\varepsilon/dt = A(e^{-B/T})(t^{-C})(\sigma^{D})$. |

$A = 4.063\ hr^{-0.366}\ MPa^{-1.715}$,
$B = 30{,}000$ K,
$C = -0.634$,
$D = 1.715$,
$T = 700$ K,
$t$ = time (hr),
$\sigma$ = stress (MPa).

*Properties of interface*

| | |
|---|---|
| Coefficient of friction | 0.33 or 1.0. |

*Properties of alumina fibers at 427°C*

| | |
|---|---|
| Elastic Modulus†† | 379 GPa, |
| Poisson Ratio†† | 0.27, |
| CTE‡‡ | 8.28 E-6°C$^{-1}$, |
| Shear Modulus | 148.9 GPa, |
| Average Strength†† | 2758 MPa,§§ |
| Weibull Modulus†† | 9. |

† Nimmer *et al.* (1989), Metals Handbook (1959).
‡ Nimmer (1989).
§ Metals Handbook (1961).
‖ Wright *et al.* (1989).
†† Deve (1992).
‡‡ Taya (1989).
§§ Strength based on 2.54 cm gauge length.